



Modeling the Inactivation of Viruses from the *Coronaviridae* Family in Response to Temperature and Relative Humidity in Suspensions or on Surfaces

Laurent Guillier,^a Sandra Martin-Latil,^b Estelle Chaix,^a Anne Thébault,^a Nicole Pavio,^c Sophie Le Poder,^c on behalf of Covid-19 Emergency Collective Expert Appraisal Group, Christophe Batéjat,^d Fabrice Biot,^e Lionel Koch,^e Donald W. Schaffner,^f Moez Sanaa^a

^aRisk Assessment Department, French Agency for Food, Environmental and Occupational Health and Safety, Maisons-Alfort, France

^bLaboratory for Food Safety, French Agency for Food, Environmental, and Occupational Health and Safety, University of Paris-EST, Maisons-Alfort, France

^cUMR Virologie 1161, ENVA, INRAE, Anses, Maisons-Alfort, France

^dEnvironment and Infectious Risks Unit, Laboratory for Urgent Response to Biological Threats (CIBU), Institut Pasteur, Paris, France

^eBacteriology Unit, French Armed Forces Biomedical Research Institute (IRBA), Brétigny-sur-Orge, France

^fDepartment of Food Science, Rutgers University, New Brunswick, New Jersey, USA

ABSTRACT Temperature and relative humidity are major factors determining virus inactivation in the environment. This article reviews inactivation data regarding coronaviruses on surfaces and in liquids from published studies and develops secondary models to predict coronaviruses inactivation as a function of temperature and relative humidity. A total of 102 *D* values (i.e., the time to obtain a log₁₀ reduction of virus infectivity), including values for severe acute respiratory syndrome coronavirus 2 (SARS-CoV-2), were collected from 26 published studies. The values obtained from the different coronaviruses and studies were found to be generally consistent. Five different models were fitted to the global data set of *D* values. The most appropriate model considered temperature and relative humidity. A spreadsheet predicting the inactivation of coronaviruses and the associated uncertainty is presented and can be used to predict virus inactivation for untested temperatures, time points, or any coronavirus strains belonging to *Alphacoronavirus* and *Betacoronavirus* genera.

IMPORTANCE The prediction of the persistence of SARS-CoV-2 on fomites is essential in investigating the importance of contact transmission. This study collects available information on inactivation kinetics of coronaviruses in both solid and liquid fomites and creates a mathematical model for the impact of temperature and relative humidity on virus persistence. The predictions of the model can support more robust decision-making and could be useful in various public health contexts. A calculator for the natural clearance of SARS-CoV-2 depending on temperature and relative humidity could be a valuable operational tool for public authorities.

KEYWORDS persistence, coronavirus, modeling, fomites, SARS-CoV-2

The pandemic of coronavirus respiratory infectious disease (COVID-19) initiated in Wuhan, China, in December 2019 was caused by an emergent virus named severe acute respiratory syndrome coronavirus 2 (SARS-CoV-2). SARS-CoV-2 belongs to the order *Nidovirales*, family *Coronaviridae*. These enveloped viruses have a positive, single-stranded RNA genome (directly translated) surrounded by a nucleocapsid protein. Coronaviruses are classified into four genera: alpha (α CoV), beta (β CoV), gamma (γ CoV), and delta (δ CoV). SARS-CoV-2 belongs to the *Betacoronavirus* genus and the *Sarbecovirus* subgenus.

Citation Guillier L, Martin-Latil S, Chaix E, Thébault A, Pavio N, Le Poder S, on behalf of Covid-19 Emergency Collective Expert Appraisal Group, Batéjat C, Biot F, Koch L, Schaffner DW, Sanaa M. 2020. Modeling the inactivation of viruses from the *Coronaviridae* family in response to temperature and relative humidity in suspensions or on surfaces. *Appl Environ Microbiol* 86:e01244-20. <https://doi.org/10.1128/AEM.01244-20>.

Editor Harold L. Drake, University of Bayreuth

Copyright © 2020 American Society for Microbiology. All Rights Reserved.

Address correspondence to Laurent Guillier, laurent.guillier@anses.fr.

Received 24 May 2020

Accepted 15 July 2020

Accepted manuscript posted online 17 July 2020

Published 1 September 2020

The route of transmission of respiratory viruses is airborne via inhalation of droplets and aerosols or through contact with contaminated intermediate objects (fomites), e.g., by self-inoculation of mucous membranes (mouth and eyes) by contaminated hands (1). The transmission route for SARS-CoV-2, SARS-CoV, and Middle East respiratory syndrome coronavirus (MERS-CoV) is primarily airborne (2–5), while environmental contamination through surfaces is uncertain (6–8). No study has currently quantified the importance of surface contact transmission in the spread of coronavirus diseases (9). Viral genomes have been detected in the stools of COVID-19 patients and sewage (10), but the role of liquid fomites has not yet been addressed.

Working with highly virulent coronavirus requires biosafety level 3 laboratory containment conditions and since SARS-CoV-2 emerged very recently, few data on its survival related to environmental conditions are available (11, 12). The use of surrogate coronaviruses has been suggested to overcome these challenges and expand the available data on coronavirus survival likelihood (13). Surrogates can be used under the assumption that they have similar physicochemical properties that mimic the viruses they represent (14, 15).

Temperature and relative humidity (RH) have been shown to impact the kinetics of inactivation of coronaviruses. Increased temperatures have been shown to increase the rate of the inactivation (11, 16), and decreased relative humidity has been associated with a reduction of coronaviruses inactivation rate on surfaces (13, 17–19). Inactivation rates were lower in suspensions than on surfaces in studies that tested both suspensions and surfaces at similar temperatures (11, 20).

Hence, the prediction of the persistence of SARS-CoV-2 on fomites is essential for the investigation of the importance of contact transmission. This study collects available information on inactivation kinetics of coronaviruses in both solid and liquid fomites and models the impact of temperature and relative humidity on virus persistence.

RESULTS

Literature review results. Table 1 shows the detailed characteristics of the 26 studies that characterized inactivation of a virus from the *Coronaviridae* family according to temperature and or relative humidity. Some kinetics were not appropriate for characterizing inactivation rate either because the duration of the experiments was too short to observe any significant decrease of virus infectivity or because the quantification limit was reached before the first time point (Table 1). A total of 102 estimates of D values (i.e., the time to obtain a \log_{10} reduction of virus infectivity) were collected from 25 of the 26 studies (see Appendix SA1 in the supplemental material). These kinetic values represent 605 individual data points. For each curve, a D value (i.e., decimal reduction time) was estimated. The 102 D values are given in Appendix SA1 in the supplemental material. Among the 102 kinetic values, 44 are from members of the *Alphacoronavirus* genus, including 1 from canine coronavirus (CCV), 2 for feline infectious peritonitis virus (FIPV), 5 for porcine epidemic diarrhea virus (PEDV), 14 for human coronavirus 229E (HCoV-229E), and 22 for porcine transmissible gastroenteritis coronavirus (TGEV). The remaining 58 kinetic values are related to the *Betacoronavirus* genus, including 2 for human coronavirus OC43 (HCoV-OC43), 2 for bovine coronavirus, 13 for murine hepatitis virus (MHV), 8 for MERS-CoV, 22 for SARS-CoV, and 11 for SARS-CoV-2. Figure 1 shows the 102 estimates of D values, including 40 values on inert surfaces and 62 values in suspension from temperatures ranging from 4 to 68°C. Different suspensions were noted, but most were laboratory media (Table 1).

Modeling inactivation. The 102 D values were fitted with five different models. Table 2 shows the performance of these models to describe D values according to temperature and relative humidity. For the tested range of temperatures (between 4 and 68°C), model 1 (the classical Bigelow model) based on a log-linear relation between D values and temperature does not perform as well as model 2 that considers a linear second-degree equation. Model 3 offers a further refinement over model 2 by also fitting the degree of the equation (n parameter). The fitted value of n was equal to 1.9

TABLE 1 Characteristics of the studies that explored inactivation of infectivity of coronavirus^a

Virus	Genus	Subgenus	Strain	Measurement	Temp (°C)	Conditions associated with treatment	Reference
BCoV	Betacoronavirus	Embecovirus	Strain 88	PFU in HRT-18 cells	4	Salad, MEM containing 2% FBS	49
CCV	Alphacoronavirus	Tegacovirus	I-71	CRFK cells (PFU)	60, 80*	MEM containing 2% FCS	50
PIPV	Alphacoronavirus	Tegacovirus	DF2-WT	Feline kidney (NLFK) cells	54	Basal medium Eagle	51
PIPV	Alphacoronavirus	Tegacovirus	ATCC-990	Crandell Reese feline kidney cell line	4†, 23	Dechlorinated, filtered tap water	52
HCoV	Alphacoronavirus	Duvinacovirus	229E	Cellular infectivity in cell strain (HDGS) W38	33, 37	Maintenance medium 2% FCS	53
HCoV	Alphacoronavirus	Duvinacovirus	229E	Cellular infectivity in lung cell line L132	21†	PBS, Earle MEM, Earle MEM + suspended cells	54
HCoV	Alphacoronavirus	Duvinacovirus	229E	Cellular infectivity in lung cell line L132	21†	Aluminum, sponge, latex at 65% RH	54
HCoV	Alphacoronavirus	Duvinacovirus	229E	CPE on MRC-5 cells	21	Teflon, PVC, rubber, steel, plastic	36
HCoV	Alphacoronavirus	Duvinacovirus	229E	MRC-5 cells (TCID ₅₀)	23	Cell culture supernatant with or without FBS	20
HCoV	Alphacoronavirus	Duvinacovirus	229E	Cellular infectivity in lung cell line L132	4†, 23	Dechlorinated, filtered tap water	52
HCoV	Alphacoronavirus	Duvinacovirus	229E	Cellular infectivity in cell strain (HDGS) W38	4†, 22, 33, 37	Earle MEM	55
HCoV	Betacoronavirus	Embecovirus	OC43	Cellular infectivity in human rectal tumor cell line HRT-18	33, 37	Maintenance medium 2% FCS	53
HCoV	Betacoronavirus	Embecovirus	OC43	Cellular infectivity in human rectal tumor cell line HRT-18	21†	PBS, Earle MEM, Earle MEM + suspended cells	54
HCoV	Betacoronavirus	Embecovirus	OC43	Cellular infectivity in human rectal tumor cell line HRT-18	21†	Aluminum, sponge*, latex* at 65% RH	54
MERS-CoV	Betacoronavirus	Sarbecovirus	FRA2	Cellular infectivity in Vero cells (TCID ₅₀)	25†, 56, 65	Cell culture supernatant	56
MERS-CoV	Betacoronavirus	Sarbecovirus	HCoV-EMC/2012	Cellular infectivity in Vero cells (TCID ₅₀)	20, 30	Plastic (30, 40, or 80% RH)	17
MERS-CoV	Betacoronavirus	Sarbecovirus	HCoV-EMC/2012	Cellular infectivity in Vero cells (TCID ₅₀)	20, 30	Plastic (30, 40, or 80% RH)	17
MHV	Betacoronavirus	Embecovirus	-	Cellular infectivity in DBT cells	4†, 25	Reagent-grade water	31
MHV	Betacoronavirus	Embecovirus	-	Cellular infectivity in DBT cells	4†, 25	Lake water	31
MHV	Betacoronavirus	Embecovirus	-	Cellular infectivity in DBT cells	4†, 20, 40	Stainless-steel surface with 20% humidity	13
MHV	Betacoronavirus	Embecovirus	-	Cellular infectivity in DBT cells	4, 20, 40	Stainless-steel surface with 50% humidity	13
MHV	Betacoronavirus	Embecovirus	-	Cellular infectivity in DBT cells	4, 20, 40	Stainless-steel surface with 80% humidity	13
MHV	Betacoronavirus	Embecovirus	MHV-2	Cellular infectivity in DBT cells (PFU)	40†, 60, 80*	MEM containing 2% FCS	50
MHV	Betacoronavirus	Embecovirus	MHV-N	Cellular infectivity in DBT cells (PFU)	40†, 60, 80*	MEM containing 2% FCS	50
MHV	Betacoronavirus	Embecovirus	A-59	Plaque assay on L2 cells	10†, 25	MEM containing 2% FCS	57
PEDV	Alphacoronavirus	Pedacovirus	V215/78	PFU on Vero cells	50	Pasteurized wastewater	58
PEDV	Alphacoronavirus	Pedacovirus	CV777	Vero cells (TCID ₅₀)	40, 44, 48	Diluted medium for virus replication	58
PEDV	Alphacoronavirus	Pedacovirus	CV777	Vero cells (TCID ₅₀)	4†, 44†, 48	MEM at pH 7.2	59
SARS-CoV	Betacoronavirus	Sarbecovirus	FFM-1	Cellular infectivity in Vero cells	56	Cell culture supernatant with or without FBS	20
SARS-CoV	Betacoronavirus	Sarbecovirus	Urbani	Cellular infectivity in Vero cells	56, 65, and 75*	Dulbecco MEM	61
SARS-CoV	Betacoronavirus	Sarbecovirus	HKU39849	Cellular infectivity in FRH-K4 (TCID ₅₀)	28, 33, 38	Plastic stored at 95% RH	62
SARS-CoV	Betacoronavirus	Sarbecovirus	HKU39849	Cellular infectivity in FRH-K4 (TCID ₅₀)	28†, 33, 38	Plastic stored at 80–89% RH	62
SARS-CoV	Betacoronavirus	Sarbecovirus	GVU6109	Cellular infectivity in Vero cells (TCID ₅₀)	20	VTM	35
SARS-CoV	Betacoronavirus	Sarbecovirus	GVU6109	Cellular infectivity in Vero cells (TCID ₅₀)	4, 20	NPA, TNS, or VTM	35
SARS-CoV	Betacoronavirus	Sarbecovirus	Tor2 (AY274119.3)	Cellular infectivity in Vero cells (TCID ₅₀)	22	Plastic and stainless steel stored at 40°C	12
SARS-CoV	Betacoronavirus	Sarbecovirus	Utah	Cellular infectivity in Vero cells (TCID ₅₀)	58, 68	Iscove 4% FCS medium	63
SARS-CoV	Betacoronavirus	Sarbecovirus	Utah	Cellular infectivity in Vero cells (TCID ₅₀)	22	Glass surface store at 10–25% RH	63
SARS-CoV	Betacoronavirus	Sarbecovirus	Hanoi	Cellular infectivity in Vero cells (TCID ₅₀)	56	MEM	64
SARS-CoV-2	Betacoronavirus	Sarbecovirus	-	Cellular infectivity in Vero cells (TCID ₅₀)	4, 22, 37, 56, 70*	VTM	11
SARS-CoV-2	Betacoronavirus	Sarbecovirus	-	Cellular infectivity in Vero cells (TCID ₅₀)	22	Plastic and stainless steel at 65% RH	11
SARS-CoV-2	Betacoronavirus	Sarbecovirus	WA1/2020 (MN985325.1)	Cellular infectivity in Vero cells (TCID ₅₀)	22	Plastic and stainless steel stored at 40°C	12
SARS-CoV-2	Betacoronavirus	Sarbecovirus	-	Cellular infectivity in Vero cells (TCID ₅₀)	56, 65*	Cell culture supernatants	65
SARS-CoV-2	Betacoronavirus	Sarbecovirus	-	Cellular infectivity in Vero cells (TCID ₅₀)	65, 95*	Nasopharyngeal samples	65
SARS-CoV-2	Betacoronavirus	Sarbecovirus	-	Cellular infectivity in Vero cells (TCID ₅₀)	56	Sera	65
TGEV	Alphacoronavirus	Tegacovirus	D52	Cellular infectivity in RPTg cells	31, 35, 39, 43, 47, 51, 55	In HEPES solution at pH 7	16
TGEV	Alphacoronavirus	Tegacovirus	D52	Cellular infectivity in RPTg cells	35, 39, 43, 47, 51	In HEPES solution at pH 8	16
TGEV	Alphacoronavirus	Tegacovirus	-	Cellular infectivity in ST cells	4†, 20, 40	Stainless steel surface with 20% RH	13
TGEV	Alphacoronavirus	Tegacovirus	-	Cellular infectivity in ST cells	4, 20, 40	Stainless steel surface with 50% RH	13
TGEV	Alphacoronavirus	Tegacovirus	-	Cellular infectivity in ST cells	4, 20, 40	Stainless steel surface with 80% RH	13
TGEV	Alphacoronavirus	Tegacovirus	-	Cellular infectivity in ST cells	4†, 25	Reagent-grade water	31
TGEV	Alphacoronavirus	Tegacovirus	-	Cellular infectivity in ST cells	4†, 25	Lake water	31

^aRH, relative humidity; VTM, viral transport medium; FCS, fetal calf serum; NPA, nasopharyngeal aspirate; TNS, throat and nasal swabs; MEM, minimal essential medium; PBS, phosphate-buffered saline; HRT, human rectal tumor; TCID₅₀, 50% tissue culture infective dose(s); HDGS, human diploid cell strain; NLFK, Norden Laboratories feline kidney; -, data not specified. Symbols: *, not included (the limit of quantification reached for the first sample time); †, not included (not enough decrease was observed during experimentation).

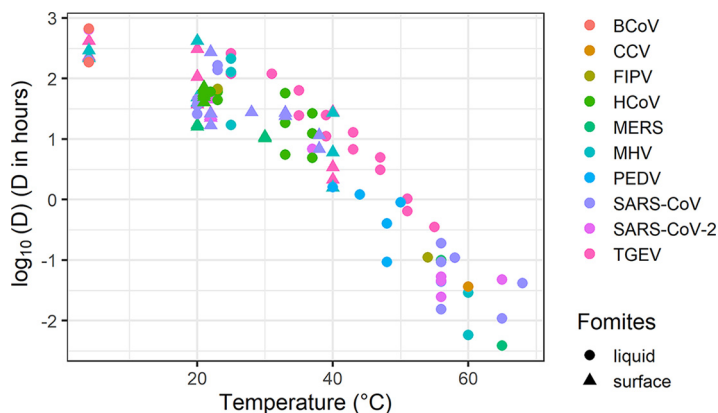


FIG 1 Decimal reduction times of 10 coronaviruses according to temperature in suspension or on inert surfaces.

with a confidence interval (CI) that includes 2 (i.e., model 2). Accordingly, the values taken by the parsimony criteria for model selection Aikaike information criterion (AIC) and Bayesian information criterion (BIC) for models 2 and 3, indicate that *n* can be set to 2.0. Figure 2 illustrates the performance of models 1 (Fig. 2A), 2 (Fig. 2B), and 3 (Fig. 2C) for which only temperature effect is considered for predicting *D* values.

Table 2 demonstrates that the inclusion of relative humidity should be considered. Models 4 and 5, which describe the *D* values according to temperature and relative humidity, were more appropriate models than models 1, 2, and 3, with a decrease of AIC of more than 2 points in comparison to other models (21). The estimated value for the shape parameter in model 5 is not different from the value 2.0. According to the BIC criterion, model 4 and model 2 were the most appropriate and undistinguishable. Based on these comparisons, model 4 was retained. Figure 3A shows the prediction of inactivation rate according to temperature and RH for this model. The high z_{RH} value (Table 2) indicates that the impact of RH is far less important than that of the temperature. For example, increasing the relative humidity by 80%, e.g., from 10 to 90%, only reduces the *D* values by a factor of 1.7. The same reduction factor of *D* values can be obtained by a small change of temperature, (e.g., changing the temperature

TABLE 2 Characteristics of the different models fitted to the 102 decimal reduction time data of coronaviruses according to temperature and relative humidity^a

Model	Fitted parameter	Best-fit value (95% CI bootstrap intervals)	Information criterion	
			Bayesian	Aikaike
1	$\text{Log}_{10}(D_{ref})$	3.1 (2.8–3.3)	–124.7	–130.0
	z_T	13.8 (12.7–15.1)		
2	$\text{Log}_{10}(D_{ref})$	2.2 (2.1–2.3)	–160.6	–165.9
	z_T	29.4 (28.4–30.5)		
3	$\text{Log}_{10}(D_{ref})$	2.3 (2.1–2.6)	–156.7	–164.6
	z_T	27.7 (23.2–31.6)		
	<i>n</i>	1.9 (1.5–2.2)		
4	$\text{Log}_{10}(D_{ref})$	2.3 (2.2–2.5)	–160.2	–168.0
	z_T	29.1 (28.1–30.1)		
	z_{RH}	341.5 (190.1–5,631.4)		
5	$\text{Log}_{10}(D_{ref})$	2.4 (2.2–2.6)	–156.2	–166.6
	z_T	27.5 (23.6–31.2)		
	z_{RH}	330.7 (182.8–7,020.1)		
	<i>n</i>	1.9 (1.6–2.2)		

^aThe temperature (T_{ref}) was set at 4°C.

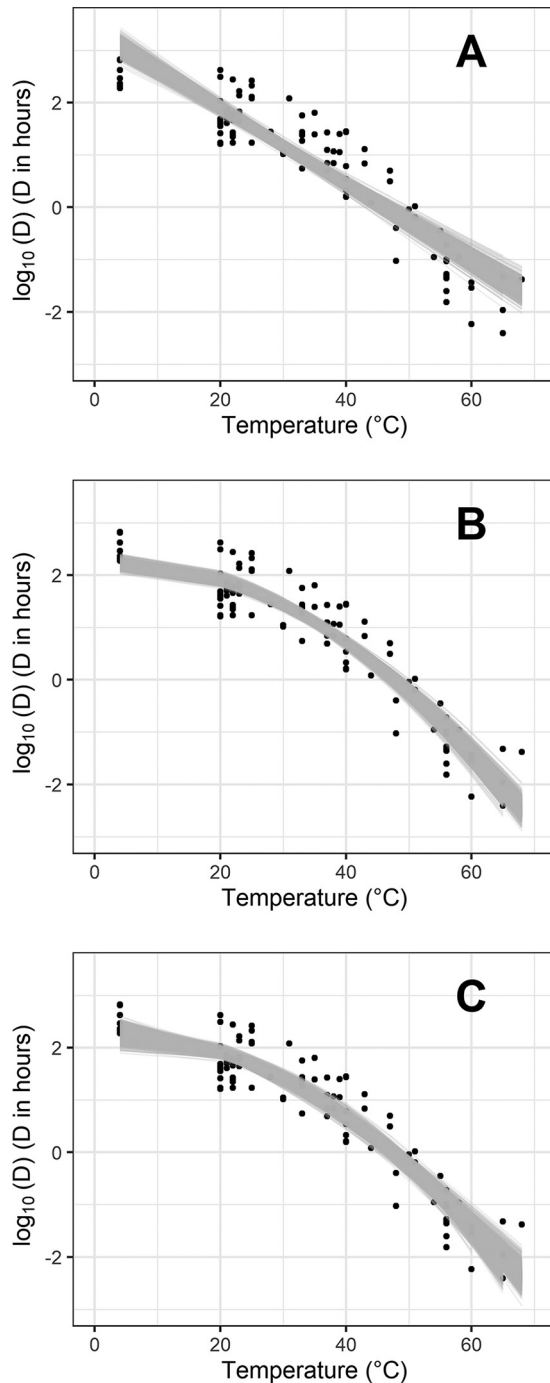


FIG 2 Observed (points) and fitted (gray lines) log decimal reduction time values according to temperature for model 1 (A), model 2 (B), and model 3 (C). One thousand (1,000) bootstrap values of uncertainty characterization are shown. Estimates of model parameters are given in Table 2.

from 10 to 15°C or from 60 to 61°C). Model 2 was retained as well since it provides very similar performance. Figure 3B shows the residuals for model 4. Comparative analyses of residuals of models 2 and 4 are provided in the supplemental material (see Fig. SA2-1 [Appendix SA2]).

Potential use of the model. An Excel spreadsheet implementing model 4 has been prepared and is available in Appendix SA3 in the supplemental material. The spreadsheet can be used to estimate the number of decimal reductions in the infectivity of coronaviruses according to user-defined time, temperature, and relative humidity. For

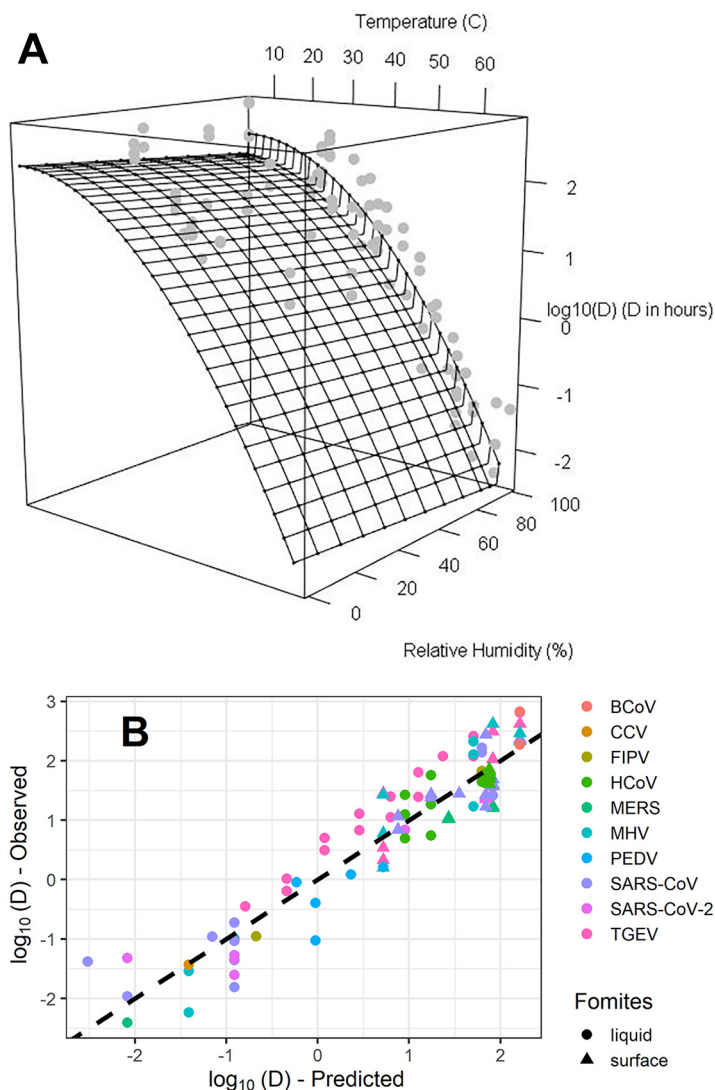


FIG 3 (A) Observed inactivation rate values (gray points) according to temperature (°C) and relative humidity (%) and model 4 surface predictions. Scatter points of observed versus predicted *D* values (*D* in hours) for model 4 (B). The dashed line represents a perfect match between observations and predictions.

example, the predicted inactivation at a temperature of 70°C for 1 min in liquid is $-11.8 \log_{10}$, with a 95% CI of -6.4 to -22.1 for model 4 and $-11.1 \log_{10}$, with a 95% CI of -5.7 to -21.4 for model 2. The spreadsheet also allows an estimate of the time necessary to reach a target number of decimal reductions of infectivity with a certain confidence level for both model 4 and model 2. For example, the time to reach a 5- \log_{10} inactivation at 20°C and 75% relative humidity is 304 h, with a 95% CI of 215 to 426 h. It will be much longer at 20% relative humidity as the time to reach a 5- \log_{10} inactivation is predicted to be 438 h, with a 95% CI of 339 to 569 h. Model 2 (which does not take into account relative humidity) provides an estimate of the time to reach a 5- \log_{10} inactivation at 20°C of 412 h, with a 95% CI of 322 to 539 h.

DISCUSSION

Our study identified 102 kinetic values for the inactivation of coronaviruses on surfaces and in suspensions. The included studies cover those identified in three recently published articles that conducted a systematic review on coronavirus inactivation (22–24). These data were used to suggest a novel inactivation model specific to

the *Coronaviridae* family. The modeling approach identified temperature and relative humidity as major factors needed to predict infectious coronavirus persistence on fomites.

The \log_{10} of D values was not linearly related to temperature in the range of temperatures studied (4 to 68°C). Bertrand et al. (15) made a similar observation in a meta-analysis for virus and phage inactivation in foods and water and proposed two different models on either side of the threshold temperature of 50°C. Laude (16) suggested a similar approach for TGEV with a threshold temperature at 45°C (16). The modeling approach we used in our study allows fitting the inactivation values with a single relation. In other meta-analyses on inactivation of viruses, Boehm et al. (25) and Hessler et al. (26) did not observe such different trends but also studied smaller temperature ranges. At the highest temperatures (>60°C), coronaviruses were found to be far less heat resistant than nonenveloped viruses (27).

The present modeling approach considers the nonmonotonous impact of relative humidity on inactivation. Coronaviruses persisted better at low RHs and at 100% RH than for intermediate RHs. Another study has confirmed that low RH makes viruses more resistant to thermal inactivation (28). Lin and Marr (29) recently observed the same relation for two bacteriophages, where the observed RH where survival was worst is close to 80%, while in the present study, the less favorable condition for coronaviruses was set to 99%. The data collected here do not cover a uniform distribution of temperatures and RH values. Further data corresponding to inactivation of coronaviruses on surfaces at low humidities for temperature between 40 and 60°C would help to refine assessment of the impact of RH. Using a worst-case RH set to 99% may be appropriate in order to estimate reductions in such situations until the model can be refined.

As noted in Materials and Methods, all of the kinetic values analyzed were established based on the quantification of coronavirus infectivity with cell cultures. The model prediction did not include other inactivation results from methods combining dyes with quantitative reverse transcription-PCR (RT-qPCR). This method (although more appropriate than classical RT-qPCR) can underestimate virus infectivity (25, 30).

The data collected from the literature does not permit models specific to species at this time. Our findings suggest that persistence potential of different coronaviruses is similar. It confirms previous finding that advocates for the use of surrogates' coronavirus such as TGEV (31). This could considerably simplify the acquisition of relevant data for persistence potential for other environmental factors. The data analyzed here only include *Alphacoronavirus* and *Betacoronavirus*, since no data for the two other major genera, *Deltacoronavirus* and *Gammacoronavirus*, were identified. Inclusion of such data would help to challenge the present model robustness.

The models developed in our study are specific to viruses from the *Coronaviridae* family. Several studies on the inactivation of other viruses have suggested that the impact of temperature can be modeled, as a whole, with a unique parameter (15, 25, 32). Variability of behavior by virus type has been observed, and model parameters to account these differences have been proposed (25, 32), e.g., nonenveloped viruses are known to show greater persistence in the environment (32). Like a recently proposed model for SARS-CoV-2 (33), our model takes into consideration relative humidity in the prediction of inactivation. This integration is of great interest from the perspective of assessing the effect of seasonality on virus persistence (34).

It is also worth noting our model is specific to fomites. Survival kinetics in fecal materials were identified (35) but not considered for inclusion. The level of matrix contamination with fecal materials has been shown to significantly increase the inactivation rate of viruses (32), so by excluding these data, model predictions are biased to be fail-safe. Inactivation data on porous surfaces were also not considered since it may be difficult to determine whether any measured inactivation is associated with real loss of infectivity or difficulty in recovering viruses absorbed inside the porous material. That said, there is no reason to consider that model predictions for coronaviruses are not pertinent to survival on porous material (e.g., face masks).

Inactivation on antimicrobial surfaces, such as copper and silver, was also not considered. For the same reason, model predictions are fail-safe since surfaces, including copper or other antimicrobial compounds, increase the inactivation rate of coronaviruses (12, 36).

The predictions of the present model could support more robust decision-making and could be useful in various contexts such as blood safety assessment (37) or validation of thermal inactivating treatments for room air, surfaces, or suspensions. Indeed, an important issue is the possibility of reusing private or public offices, hotel rooms, or vehicles that are difficult to decontaminate. Moreover, many devices, such as electronics or more sensitive materials, are not suitable for chemical decontamination processes which could make them inoperative. Another aspect of decontamination is the economical challenge since large-scale decontamination of buildings can cost billions of dollars (38). Furthermore, the use of detergents and/or disinfectants may have environmental consequences. Thus, the large-scale SARS-CoV-2 decontamination of surfaces that are not necessarily in contact with people may not be required. For these reasons, the waiting time needed before handling suspected contaminated materials in the absence of decontamination is more than ever an important question. A calculator for the natural clearance of SARS-CoV-2 depending on temperature could be a valuable operational tool for public authorities (33).

The present model also opens the way for risk assessment for SARS-CoV-2 transmission through contact (39). Further model developments, including data on matrix pH, salinity, and exposure to visible and UV light, would also be important to consider (32, 40).

MATERIALS AND METHODS

Selection of the studies. Four inclusion criteria were used to identify studies that characterized inactivation of coronaviruses according to temperature and relative humidity. Selected studies had to focus on one virus from the *Coronaviridae* family. Inactivation must have been carried out in suspensions or on inert nonporous surfaces. Only surfaces without antimicrobial properties were considered. The quantification of infectious viruses had to be assessed by cell culture, since RT-qPCR can underestimate actual virus infectivity (25, 30). Finally, the available kinetic data points should be sufficient to allow precise statistical estimation of the rate of viral inactivation without bias. In this context, kinetic data with no significant inactivation observed during the experiment or with values below the quantification limit in the first time interval were not included.

Data collection. The kinetics were gathered from either the figures or the tables of the selected studies. The digitize R package (41) was used to retrieve data from scatterplots in figures. This package loads a graphical file of a scatterplot (in jpeg format) in the graphical window of R and calibrates and extracts the data. Data were manually reported in R vector for data provided in tables. A key was attributed to kinetics collected in each study (Table 1). Specific lists of tables and figures used for each kinetics study are given in Appendix SA1 in the supplemental material.

Modeling of inactivation. A simple primary model was used for describing the inactivation kinetics. The D values (or decimal reduction times) were determined from the kinetics of the \log_{10} number of infectious viruses (N) over time (t) at each experimental temperature. D is the inverse of the slope of the inactivation kinetics:

$$\log_{10}(N) = \log_{10}(N_0) - \frac{t}{D} \quad (1)$$

Several secondary models describing the impact of temperature (T) and relative humidity (RH) on D values were tested. The gamma concept of inactivation was used (42, 43). In this approach, the inactivation of a microbial population could be estimated by:

$$\log_{10}(D) = \log_{10}(D_{ref}) - \sum \log_{10}(\lambda_{xi}(x_i)) \quad (2)$$

where λ_{xi} quantifies the influence of each environmental factor (x_i corresponds to temperature and relative humidity in this study) on the microbial resistance (D_{ref}) observed in reference conditions.

Based on equation 2, five different secondary models were established. Models 1, 2, and 3 do not consider the nature of the fomite.

Model 1 is the classical Bigelow model (44). It models only the effect of temperature. The z_T , the increase of temperature which leads to a 10-fold reduction of D , value was determined as the negative inverse slope of the plot of $\log_{10}(D)$ versus temperature. z_T is the increase of temperature which leads to a 10-fold reduction of the decimal reduction time. T_{ref} is the reference temperature (set to 4°C in our study) and $\log_{10}(D_{ref})$ is the $\log_{10}(D)$ at T_{ref} . Model 1 is as follows:

$$\log_{10}(\lambda_T(T)) = \frac{T - T_{ref}}{z} \text{ and } \log_{10}(\lambda_{RH}(RH)) = 0$$

Model 2 considers the effect of temperature; however, D values were fitted according to temperature using a semilog approach, derived from Mafart (43):

$$\log_{10}(\lambda_T(T)) = \left(\frac{T - T_{ref}}{Z_T}\right)^2 \text{ and } \log_{10}(\lambda_{RH}(RH)) = 0$$

Model 3 is similar to model 2, but the shape parameter n was estimated instead of being set to 2:

$$\log_{10}(\lambda_T(T)) = \left(\frac{T - T_{ref}}{Z_T}\right)^n \text{ and } \log_{10}(\lambda_{RH}(RH)) = 0$$

The last two models (i.e., models 4 and 5) consider the effect of temperature and the nature of the fomites. The type of fomite was taken into account through the use of relative humidity. Suspensions correspond to more than 99% RH conditions while surfaces are associated with RH conditions below this threshold. The models consider that surfaces at higher relative humidity allow for more rapid inactivation and that inactivation in suspensions is equivalent to inactivation on surfaces exposed to low RH. In model 4, the shape parameter for temperature was set to 2 as in model 2.

$$\log_{10}(\lambda_T(T)) = \left(\frac{T - T_{ref}}{Z_T}\right)^2 \text{ and}$$

$$\log_{10}(\lambda_{RH}(RH)) = \begin{cases} \frac{RH}{z_{RH}} & RH < 99\% \\ 0 & RH \geq 99\% \end{cases}$$

In model 5, n is a model parameter to be estimated:

$$\log_{10}(\lambda_T(T)) = \left(\frac{T - T_{ref}}{Z_T}\right)^n \text{ and}$$

$$\log_{10}(\lambda_{RH}(RH)) = \begin{cases} \frac{RH}{z_{RH}} & RH < 99\% \\ 0 & RH \geq 99\% \end{cases}$$

In models 4 and 5, z_{RH} is the increase in relative humidity which leads to a 10-fold reduction of the decimal reduction time.

Model parameter estimation. The model's parameters were fitted with `nls()` R function. Confidence intervals of fitted parameters were assessed by bootstrap using `nlsBoot()` function from `nlsMicrobio` R package (45). The five models were compared according to penalized-likelihood criteria, the Akaike information criterion (AIC) (46) and the Bayesian information criterion (BIC) (47):

$$AIC = p \cdot \ln\left(\frac{RSS}{p}\right) + 2k$$

$$BIC = p \cdot \ln\left(\frac{RSS}{p}\right) + k \cdot \ln(p)$$

where RSS is the residual sum of squares, p is the number of experimental points, and k the number of parameters in the model. The lower the AIC and BIC, the better the model fits the data set.

Data availability. Detailed information in the tables and figures indicating where the data were collected is provided in Appendix SA1 in the supplemental material. All scripts and data used to prepare figures and tables of the manuscript are available in a Github repository (<https://github.com/lguillier/Persistence-Coronavirus>) (48).

SUPPLEMENTAL MATERIAL

Supplemental material is available online only.

SUPPLEMENTAL FILE 1, XLSX file, 0.02 MB.

SUPPLEMENTAL FILE 2, PDF file, 0.4 MB.

SUPPLEMENTAL FILE 3, XLSX file, 0.3 MB.

ACKNOWLEDGMENTS

The Covid-19 Emergency Collective Expert Appraisal Group members included the coauthors L.G., S.M.-L., E.C., N.P., S.L.P., and M.S., as well as (in alphabetical order) Paul Brown, Charlotte Dunoyer, Florence Etoire, Elissa Khamisse, Meriadeg Le Gouil, François Meurens, Gilles Meyer, Elodie Monchatre-Leroy, Gaëlle Simon, and Astrid Vabret.

REFERENCES

1. Kutter JS, Spronken MI, Fraaij PL, Fouchier RA, Herfst S. 2018. Transmission routes of respiratory viruses among humans. *Curr Opin Virol* 28: 142–151. <https://doi.org/10.1016/j.coviro.2018.01.001>.
2. Lu J, Gu J, Li K, Xu C, Su W, Lai Z, Zhou D, Yu C, Xu B, Yang Z. 2020. COVID-19 outbreak associated with air conditioning in restaurant, Guangzhou, China, 2020. *Emerg Infect Dis* 26:1628–1631. <https://doi.org/10.3201/eid2607.200764>.
3. Lee N, Hui D, Wu A, Chan P, Cameron P, Joynt GM, Ahuja A, Yung MY,

- Leung CB, To KF, Lui SF, Szeto CC, Chung S, Sung JY. 2003. A major outbreak of severe acute respiratory syndrome in Hong Kong. *N Engl J Med* 348:1986–1994. <https://doi.org/10.1056/NEJMoa030685>.
4. Kim S-H, Chang SY, Sung M, Park JH, Bin Kim H, Lee H, Choi J-P, Choi WS, Min J-Y. 2016. Extensive viable Middle East respiratory syndrome (MERS) coronavirus contamination in air and surrounding environment in MERS isolation wards. *Clin Infect Dis* 63:363–369. <https://doi.org/10.1093/cid/ciw239>.
 5. Liu J, Liao X, Qian S, Yuan J, Wang F, Liu Y, Wang Z, Wang F, Liu L, Zhang Z. 2020. Community transmission of severe acute respiratory syndrome coronavirus 2, Shenzhen, China, 2020. *Emerg Infect Dis* 26:1320–1323. <https://doi.org/10.3201/eid2606.200239>.
 6. Chen Y-C, Huang L-M, Chan C-C, Su C-P, Chang S-C, Chang Y-Y, Chen M-L, Hung C-C, Chen W-J, Lin F-Y, Lee Y-T, SARS Research Group of National Taiwan University College of Medicine and National Taiwan University Hospital. 2004. SARS in hospital emergency room. *Emerg Infect Dis* 10:782–788. <https://doi.org/10.3201/eid1005.030579>.
 7. Danis K, Epaulard O, Bénet T, Gaymard A, Campoy S, Botelho-Nevers E, Bouscambert-Duchamp M, Spacciferri G, Ader F, Mailles A, Boudalaa Z, Tolsma V, Berra J, Vaux S, Forestier E, Landelle C, Fougere E, Thabuis A, Berthelot P, Veil R, Levy-Bruhl D, Chidiac C, Lina B, Coignard B, Saura C, Brottet E, Casamatta D, Gallien Y, George S, Viriot D, Ait Belghiti F, Bernard-Stoecklin S, Descenclos J-C, et al. 2020. Cluster of coronavirus disease 2019 (Covid-19) in the French Alps, 2020. *Clin Infect Dis* <https://doi.org/10.1093/cid/ciaa424>.
 8. Otter JA, Donskey C, Yezli S, Douthwaite S, Goldenberg SD, Weber DJ. 2016. Transmission of SARS and MERS coronaviruses and influenza virus in healthcare settings: the possible role of dry surface contamination. *J Hosp Infect* 92:235–250. <https://doi.org/10.1016/j.jhin.2015.08.027>.
 9. Wolff MH, Sattar SA, Adegunrin O, Tetro J. 2005. Environmental survival and microbicidal inactivation of coronaviruses, p 201–212. *In* Coronaviruses with special emphasis on first insights concerning SARS. Springer, New York, NY.
 10. Medema G, Heijnen L, Elsinga G, Italiaander R, Brouwer A. 2020. Presence of SARS-coronavirus-2 in sewage. medRxiv <https://doi.org/10.1101/2020.03.29.20045880>.
 11. Chin A, Chu J, Perera M, Hui K, Yen H-L, Chan M, Peiris M, Poon L. 2020. Stability of SARS-CoV-2 in different environmental conditions. *Lancet Microbe* 1:e10. [https://doi.org/10.1016/S2666-5247\(20\)30003-3](https://doi.org/10.1016/S2666-5247(20)30003-3).
 12. van Doremalen N, Bushmaker T, Morris DH, Holbrook MG, Gable A, Williamson BN, Tamin A, Harcourt J, Thornhorn NJ, Thorne G, Gerber SL, Lloyd-Smith JO, de Wit E, Munster VJ. 2020. Aerosol and surface stability of SARS-CoV-2 as compared with SARS-CoV-1. *N Engl J Med* 382:1564–1567. <https://doi.org/10.1056/NEJMc2004973>.
 13. Casanova LM, Jeon S, Rutala WA, Weber DJ, Sobsey MD. 2010. Effects of air temperature and relative humidity on coronavirus survival on surfaces. *Appl Environ Microbiol* 76:2712–2717. <https://doi.org/10.1128/AEM.02291-09>.
 14. Bozkurt H, D'Souza DH, Davidson PM. 2015. Thermal inactivation kinetics of human norovirus surrogates and hepatitis A virus in turkey deli meat. *Appl Environ Microbiol* 81:4850–4859. <https://doi.org/10.1128/AEM.00874-15>.
 15. Bertrand I, Schijven JF, Sánchez G, Wyn-Jones P, Ottoson J, Morin T, Muscillo M, Verani M, Nasser A, de Roda Husman AM, Myrmet M, Sellwood J, Cook N, Gantzer C. 2012. The impact of temperature on the inactivation of enteric viruses in food and water: a review. *J Appl Microbiol* 112:1059–1074. <https://doi.org/10.1111/j.1365-2672.2012.05267.x>.
 16. Laude H. 1981. Thermal inactivation studies of a coronavirus, transmissible gastroenteritis virus. *J Gen Virol* 56:235–240. <https://doi.org/10.1099/0022-1317-56-2-235>.
 17. Van Doremalen N, Bushmaker T, Munster V. 2013. Stability of Middle East respiratory syndrome coronavirus (MERS-CoV) under different environmental conditions. *Eurosurveillance* 18:20590. <https://doi.org/10.2807/1560-7917.ES2013.18.38.20590>.
 18. Ijaz M, Brunner A, Sattar S, Nair RC, Johnson-Lussenburg C. 1985. Survival characteristics of airborne human coronavirus 229E. *J Gen Virol* 66:2743–2748. <https://doi.org/10.1099/0022-1317-66-12-2743>.
 19. Ijaz M, Karim Y, Sattar S, Johnson-Lussenburg C. 1987. Development of methods to study the survival of airborne viruses. *J Virol Methods* 18:87–106. [https://doi.org/10.1016/0166-0934\(87\)90114-5](https://doi.org/10.1016/0166-0934(87)90114-5).
 20. Rabenau H, Cinatl J, Morgenstern B, Bauer G, Preiser W, Doerr H. 2005. Stability and inactivation of SARS coronavirus. *Med Microbiol Immunol* 194:1–6. <https://doi.org/10.1007/s00430-004-0219-0>.
 21. Burnham KP, Anderson DR. 1998. Practical use of the information-theoretic approach, p 75–117. *In* Model selection and inference. Springer, New York, NY.
 22. Kampf G, Voss A, Scheithauer S. 2020. Inactivation of coronaviruses by heat. *J Hosp Infect* 105:348–349. <https://doi.org/10.1016/j.jhin.2020.03.025>.
 23. La Rosa G, Bonadonna L, Lucentini L, Kenmoe S, Suffredini E. 2020. Coronavirus in water environments: occurrence, persistence and concentration methods: a scoping review. *Water Res* 179:115899. <https://doi.org/10.1016/j.watres.2020.115899>.
 24. Kampf G, Todt D, Pfaender S, Steinmann E. 2020. Persistence of coronaviruses on inanimate surfaces and its inactivation with biocidal agents. *J Hosp Infect* 104:246–251. <https://doi.org/10.1016/j.jhin.2020.01.022>.
 25. Boehm AB, Silverman AI, Schriever A, Goodwin K. 2019. Systematic review and meta-analysis of decay rates of waterborne mammalian viruses and coliphages in surface waters. *Water Res* 164:114898. <https://doi.org/10.1016/j.watres.2019.114898>.
 26. Hesslering M, Hoenes K, Lingenfelder C. 2020. Selection of parameters for thermal coronavirus inactivation: a data-based recommendation. *GMS Hyg Infect Control* 15:Doc16. <https://doi.org/10.3205/dgkh000351>.
 27. Firquet S, Beaujard S, Lobert P-E, Sané F, Caloone D, Izard D, Hober D. 2014. Viruses contained in droplets applied on warmed surface are rapidly inactivated. *Microbes Environ* 29:408–412. <https://doi.org/10.1264/jsm.2.ME14108>.
 28. Sauerbrei A, Wutzler P. 2009. Testing thermal resistance of viruses. *Arch Virol* 154:115–119. <https://doi.org/10.1007/s00705-008-0264-x>.
 29. Lin K, Marr LC. 2020. Humidity-dependent decay of viruses, but not bacteria, in aerosols and droplets follows disinfection kinetics. *Environ Sci Technol* 54:1024–1032. <https://doi.org/10.1021/acs.est.9b04959>.
 30. Coudray-Meunier C, Fraise A, Martin-Latil S, Guillier L, Perelle S. 2013. Discrimination of infectious hepatitis A virus and rotavirus by combining dyes and surfactants with RT-qPCR. *BMC Microbiol* 13:216. <https://doi.org/10.1186/1471-2180-13-216>.
 31. Casanova L, Rutala WA, Weber DJ, Sobsey MD. 2009. Survival of surrogate coronaviruses in water. *Water Res* 43:1893–1898. <https://doi.org/10.1016/j.watres.2009.02.002>.
 32. Brainard J, Pond K, Hunter PR. 2017. Censored regression modeling to predict virus inactivation in wastewaters. *Environ Sci Technol* 51:1795–1801. <https://doi.org/10.1021/acs.est.6b05190>.
 33. U.S. Department of Homeland Security. 2020. SARS-CoV-2 indoor environmental stability predictive model. U.S. Department of Homeland Security, Washington, DC. https://www.dhs.gov/sites/default/files/publications/sars-cov-2_environment_predictive_model_factsheet_2.pdf.
 34. Prussin AJ, Schwake DO, Lin K, Gallagher DL, Buttling L, Marr LC. 2018. Survival of the enveloped virus Phi6 in droplets as a function of relative humidity, absolute humidity, and temperature. *Appl Environ Microbiol* 84:e00551-18. <https://doi.org/10.1128/AEM.00551-18>.
 35. Lai MY, Cheng PK, Lim WW. 2005. Survival of severe acute respiratory syndrome coronavirus. *Clin Infect Dis* 41:e67–e71. <https://doi.org/10.1086/433186>.
 36. Warnes SL, Little ZR, Keevil CW. 2015. Human coronavirus 229E remains infectious on common touch surface materials. *mBio* 6:e01697-15. <https://doi.org/10.1128/mBio.01697-15>.
 37. Chang L, Yan Y, Wang L. 2020. Coronavirus disease 2019: coronaviruses and blood safety. *Transfus Med Rev* 34:75–80. <https://doi.org/10.1016/j.tmr.2020.02.003>.
 38. Schmitt K, Zaccchia NA. 2012. Total decontamination cost of the anthrax letter attacks. *Biosecur Bioterror* 10:98–107. <https://doi.org/10.1089/bsp.2010.0053>.
 39. Haas C. 2020. Coronavirus and risk analysis. *Risk Anal* 40:660–661. <https://doi.org/10.1111/risa.13481>.
 40. Hesslering M, Hönes K, Vatter P, Lingenfelder C. 2020. Ultraviolet irradiation doses for coronavirus inactivation: review and analysis of coronavirus photoinactivation studies. *GMS Hyg Infect Control* 15:Doc08. <https://doi.org/10.3205/dgkh000343>.
 41. Poisot T. 2011. The digitize package: extracting numerical data from scatterplots. *R J* 3:25–26. <https://doi.org/10.32614/RJ-2011-004>.
 42. Coroller L, Kan-King-Yu D, Leguerinel I, Mafart P, Membré J-M. 2012. Modelling of growth, growth/no-growth interface and nonthermal inactivation areas of *Listeria* in foods. *Int J Food Microbiol* 152:139–152. <https://doi.org/10.1016/j.jfoodmicro.2011.09.023>.
 43. Mafart P. 2000. Taking injuries of surviving bacteria into account for optimising heat treatments. *Int J Food Microbiol* 55:175–179. [https://doi.org/10.1016/S0168-1605\(00\)00160-4](https://doi.org/10.1016/S0168-1605(00)00160-4).

44. Bigelow W. 1921. The logarithmic nature of thermal death time curves. *J Infect Dis* 29:528–536. <https://doi.org/10.1093/infdis/29.5.528>.
45. Baty F, Delignette-Muller M. 2017. nlsMicrobio: data sets and nonlinear regression models dedicated to predictive microbiology. R package version 0.0-1 <https://CRAN.R-project.org/package=nlsMicrobio>.
46. Akaike H. 1974. A new look at the statistical model identification. *IEEE Trans Automat Contr* 19:716–723. <https://doi.org/10.1109/TAC.1974.1100705>.
47. Schwarz G. 1978. Estimating the dimension of a model. *Ann Statist* 6:461–464. <https://doi.org/10.1214/aos/1176344136>.
48. Guillier L. 2020. Data and models related to coronavirus inactivation. <https://doi.org/10.5281/zenodo.3946715>.
49. Mullis L, Saif LJ, Zhang Y, Zhang X, Azevedo MS. 2012. Stability of bovine coronavirus on lettuce surfaces under household refrigeration conditions. *Food Microbiol* 30:180–186. <https://doi.org/10.1016/j.fm.2011.12.009>.
50. Saknimit M, Inatsuki I, Sugiyama Y, Yagami K. 1988. Virucidal efficacy of physicochemical treatments against coronaviruses and parvoviruses of laboratory animals. *Jikken Dobutsu Exp Dobutsu* 37:341–345. https://doi.org/10.1538/expanim1978.37.3_341.
51. Christianson K, Ingersoll J, Landon R, Pfeiffer N, Gerber J. 1989. Characterization of a temperature sensitive feline infectious peritonitis coronavirus. *Arch Virol* 109:185–196. <https://doi.org/10.1007/BF01311080>.
52. Gundy PM, Gerba CP, Pepper IL. 2009. Survival of coronaviruses in water and wastewater. *Food Environ Virol* 1:10. <https://doi.org/10.1007/s12560-008-9001-6>.
53. Bucknall RA, King LM, Kapikian AZ, Chanock RM. 1972. Studies with human coronaviruses II. Some properties of strains 229E and OC43. *Proc Soc Exp Biol Med* 139:722–727. <https://doi.org/10.3181/00379727-139-36224>.
54. Sizon J, Yu M, Talbot P. 2000. Survival of human coronaviruses 229E and OC43 in suspension and after drying on surfaces: a possible source of hospital-acquired infections. *J Hosp Infect* 46:55–60. <https://doi.org/10.1053/jhin.2000.0795>.
55. Lamarre A, Talbot PJ. 1989. Effect of pH and temperature on the infectivity of human coronavirus 229E. *Can J Microbiol* 35:972–974. <https://doi.org/10.1139/m89-160>.
56. Leclercq I, Batejat C, Burguière AM, Manuguerra JC. 2014. Heat inactivation of the Middle East respiratory syndrome coronavirus. *Influenza Other Respir Viruses* 8:585–586. <https://doi.org/10.1111/irv.12261>.
57. Ye Y, Ellenberg RM, Graham KE, Wigginton KR. 2016. Survivability, partitioning, and recovery of enveloped viruses in untreated municipal wastewater. *Environ Sci Technol* 50:5077–5085. <https://doi.org/10.1021/acs.est.6b00876>.
58. Hofmann M, Wyler R. 1989. Quantitation, biological, and physicochemical properties of cell culture-adapted porcine epidemic diarrhea coronavirus (PEDV). *Vet Microbiol* 20:131–142. [https://doi.org/10.1016/0378-1135\(89\)90036-9](https://doi.org/10.1016/0378-1135(89)90036-9).
59. Quist-Rybachuk G, Nauwynck H, Kalmar I. 2015. Sensitivity of porcine epidemic diarrhea virus (PEDV) to pH and heat treatment in the presence or absence of porcine plasma. *Vet Microbiol* 181:283–288. <https://doi.org/10.1016/j.vetmic.2015.10.010>.
60. Hulst MM, Heres L, Hakze-van der Honing R, Pelsler M, Fox M, van der Poel WH. 2019. Study on inactivation of porcine epidemic diarrhoea virus, porcine sapelovirus 1 and adenovirus in the production and storage of laboratory spray-dried porcine plasma. *J Appl Microbiol* 126:1931–1943. <https://doi.org/10.1111/jam.14235>.
61. Darnell ME, Subbarao K, Feinstone SM, Taylor DR. 2004. Inactivation of the coronavirus that induces severe acute respiratory syndrome, SARS-CoV. *J Virol Methods* 121:85–91. <https://doi.org/10.1016/j.jviromet.2004.06.006>.
62. Chan K, Peiris J, Lam S, Poon L, Yuen K, Seto W. 2011. The effects of temperature and relative humidity on the viability of the SARS coronavirus. *Adv Virol* 2011:734690. <https://doi.org/10.1155/2011/734690>.
63. Pagat A-M, Seux-Goepfert R, Lutsch C, Lecouturier V, Saluzzo J-F, Kusters IC. 2007. Evaluation of SARS-coronavirus decontamination procedures. *Appl Biosaf* 12:100–108. <https://doi.org/10.1177/153567600701200206>.
64. Kariwa H, Fujii N, Takashima I. 2006. Inactivation of SARS coronavirus by means of povidone-iodine, physical conditions, and chemical reagents. *Dermatology* 212:119–123. <https://doi.org/10.1159/000089211>.
65. Batejat C, Grassin Q, Manuguerra J-C, Leclercq I. 2020. Heat inactivation of the severe acute respiratory syndrome coronavirus 2. *bioRxiv* <https://doi.org/10.1101/2020.05.01.067769>.